Dalton Transactions

Accepted Manuscript

This is an *Accepted Manuscript*, which has been through the Royal Society of Chemistry peer review process and has been accepted for publication.

Accepted Manuscripts are published online shortly after acceptance, before technical editing, formatting and proof reading. Using this free service, authors can make their results available to the community, in citable form, before we publish the edited article. We will replace this *Accepted Manuscript* with the edited and formatted *Advance Article* as soon as it is available.

You can find more information about *Accepted Manuscripts* in the Information for Authors.

Please note that technical editing may introduce minor changes to the text and/or graphics, which may alter content. The journal's standard Terms & Conditions and the Ethical guidelines still apply. In no event shall the Royal Society of Chemistry be held responsible for any errors or omissions in this *Accepted Manuscript* or any consequences arising from the use of any information it contains.

ROYAL SOCIETY OF CHEMISTRY

www.rsc.org/dalton

Table of Contents Graphic

Synthesis and characterization of pyridazine-based iron chelators

Yongmin Ma, Xiaole Kong, Yu-lin Chen, Robert C Hider

New pyridazine-based iron chelators were synthesized from 3,4,5-trichloropyridazine via a 6-step reaction and their iron affinity constants are characterized.

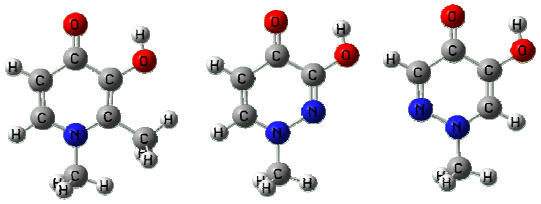

Dalton Transactions Accepted Manuscript

Synthesis and characterizations of pyridazine-based iron chelators

Yongmin Ma[a], Xiaole Kong[b], Yu-lin Chen[a], Robert C Hider[b*]

[a]College of Pharmaceutical Science, Zhejiang Chinese Medical University, Hangzhou, Zhejiang, P R China, 310053

[b]Department of Pharmacy, King's College London, Franklin-Wilkins Building, 150 Stamford Street, London, SE1 9NH, UK

Abstract

In an attempt to design ligands which require both a high iron(III) affinity and a low iron(II) affinity, the 3-hydroxypyridin-4-one structure has been modified to introduce an additional nitrogen atom in the pyridine ring to form a pyridazine. The target molecules were synthesized from a chlorine-substituted pyridazine using step-by-step methoxylations. A total of six 3- and 5-hydroxypyridazin-4(1H)-ones have been synthesized, with a methyl, ethyl or n-propyl group on the N1 of the pyridazine ring. In the reaction of the pyridazines with alkyl iodide, the presence of acetone drives the reaction to afford pyridazinones rather than the desired pyridaziniums. The *pKa* values of the free ligands , the stability constants of their iron(III) complexes and corresponding pFe^{III} values demonstrate that this type of ligand has lower values when compared with those of deferiprone. The reduction potential values of the iron complexes obtained from cyclic voltammetry measurements, are used to determine the corresponding pFe^{II} values. Although two compounds of the **20** series have marginally higher $\log\beta_3(Fe^{III})/\log\beta_3(Fe^{II})$ ratios than those of deferiprone, they possess pFe^{III} values < 20, indicating that this type of chelator is unlikely to be optimized into a useful therapeutic agent.

*To whom correspondence should be addressed: Email: robert.Hider@kcl.ac.uk; Fax: (+44) 20 7848 4800

Dalton Transactions Accepted Manuscript

Introduction

Much has been written about the design of therapeutically useful iron chelators[1, 2]. It is generally accepted that such compounds should be designed such that they selectively bind iron(III) and have a minimal tendency to inhibit metalloenzymes and in particular iron-dependent enzymes. For efficient scavenging of iron they should possess a pFe^{III} value $\geqslant$ 20. In general, hydroxypyridinones have low inhibitory effects on haem- and iron-sulphur cluster-containing enzymes. However, some iron(II)-dependent enzymes, for instance the nonhaem dioxygenases[3, 4], do not bind iron tightly and the enzyme iron complexes are kinetically labile. If a chelator binds iron(II) tightly, it will inhibit this group of enzymes by scavenging the hexaaquo iron(II) or glutathione iron(II) complex species present in the cytoplasm[5]. Clearly this competition should be avoided if at all possible. The range of affinities for iron(II) for this nonhaem dioxygenase enzyme group is 0.05 - 2 μM.[6] As the cytoplasmic concentration range for iron(II) falls in the range 0.2 - 5 μM[7-9], depending on the cell type, the enzymes may not be fully saturated with iron(II). Indeed the iron(II) levels can in principle control the activity of the enzyme[4, 6]. If a therapeutic chelator is capable of binding cytoplasmic iron(II) and as a result reduces the level to 0.01 μM, the activity of a wide range of enzymes, important for controlling the rate of transcription would be affected[6]. Consequently we wish to design ligands which possess a high affinity for iron(III) (pFe^{III} $\geqslant$ 20) while maintaining a low affinity for iron(II), pFe^{II} in the range 6.000-6.005. Such values indicate a low affinity for iron(II), a pFe^{II} value of 6 indicates absence of iron(II) binding. pFe^{III} values are equal to $-\log[Fe^{III}]^{3+}$ under defined conditions. In this work pFe^{III} is calculated for $[Fe^{III}]_{total}$ = 1 μM; $[Ligand]_{total}$ = 10 μM at pH 7.4 and pFe^{II} is calculated for $[Fe^{II}]_{total}$ = 1 μM; $[Ligand]_{total}$ = 100 μM at pH 7.4. The clinically used iron chelator, deferiprone[10], possesses a pFe^{II} value of 6.008, which is slightly higher than the ideal range. Thus we wish to optimise the 3-hydroxypyridin-4-one structure such that we can achieve parameters equal or close to the values of the "target" zone in Figure 1, together with suitable partition coefficients and molecular size.

Deferiprone (**1**) possesses two *pKa* values, 3.7 and 9.8, assigned to the 4- and 3-hydroxyl groups respectively[11]. The low *pKa* value of the 4-hydroxyl function of deferiprone results from the delocalisation of the negative charge on 4-oxygen across the ring to the

Dalton Transactions Accepted Manuscript

ring nitrogen cation (Scheme 1). In order to modify the *pKa* value of 3-hydroxyl of deferiprone (**1**), and thereby also modify the logβ_3 values of both the iron(III) and iron(II) complexes, we have designed molecules where either the ring C2 or C6 of deferiprone is replaced by a nitrogen atom (**2** and **3**) in order to stabilise the resulting 3-oxygen anion. This series of compounds all form non charged 3:1 (ligand:iron) complexes as typified by iron$^{(III)}$ (deferiprone)$_3$ (**4**) (Fig. 2).

Synthesis

The synthetic route of the 3(5)-hydroxypyridazin-4(1H)-ones adopted in this study is summarized in Scheme 2. We initially attempted to convert commercially available 4,5-dichloropyridazin-3-ol (**5**) directly into a 4-methoxy substituted derivative, a potential chelator precursor, by reacting with sodium methoxide. It was expected that two isomers would be produced, as both 4- and 5-chloro atoms can be replaced by the methoxide anion. Unfortunately, only the 5-OMe substituted analogue was obtained (route a). This phenomenon may be due to the spatial hindrance of the 4-chloro by the *ortho*- chloro and hydroxyl groups. We then attempted to protect the 3-hydroxyl group of compound **5** using K_2CO_3/MeI reagents. However, the nitrogen of the pyridazine ring was methylated in preference to the 3-hydroxyl group (route b). We therefore carried on the reaction of compound **5** with phosphorus oxychloride to obtain 3,4,5-trichloropyridazine **8** (route c), followed by step-by-step methoxylations.[12] Monomethoxylation of compound **8** with equimolar sodium methoxide at room temperature afforded a mixture of 4-methoxy- and 5-methoxy- monosubstituted derivatives **9** and **10** at 32% and 53% respectively and a tiny amount of the 3-methoxy analogue, which is in agreement with previously reported data[12]. The monomethoxy compounds **9** and **10** were further methoxylated with an equimolar amount of NaOMe under reflux conditions to give the dimethoxy compounds **11** (minor) and **12** (major), **12** (minor) and **13** (major), respectively. On the basis of the above results, we can conclude that the reactivity of the three chlorine atoms of the multichloropyridazines is 5 > 4 > 3. However, once one chlorine atom has been exchanged with a methoxy group, a second methoxy group prefers to attach at the *meta*-position due to the spatial hindrance, such as observed in reaction of **10** with NaOMe to obtain the main product **13**.

Dalton Transactions Accepted Manuscript

The dimethoxy compounds **11** and **12** were hydrogenated over $Pd(OH)_2/Et_3N$ in EtOAc to quantitatively afford colorless crystals **14** and **15** respectively. ^{1}H NMR spectra clearly demonstrated doublet peaks for C_5-H and C_6-H of compound **14** with coupling constants at 5.3 Hz and a singlet peak for C_3-H and C_6-H (identical) of compound **15**. Furthermore, doublet peaks were found for C_4-H and C_6-H of the hydrogenation product of compound **13**, with coupling constants at 2.5 Hz, smaller than those of compound **14**. These NMR data confirm the structures of the methoxylation products.

Compounds **14** and **15** were reacted with alkyl iodide in the absence of solvent to form the pyridazinium compounds **16** and **17** respectively. In each case only one alkyl group was attached to one of the two nitrogen atoms on the ring. Due to steric hindrance of the 3-methoxy group, the alkyl function was expected to be attached on 3,4-methoxypyridazine **14** at N1 rather than N2. To confirm this result, we carried out a NOESY experiment with the product. In the ^{1}H NMR spectrum for the methylated product of **14**, there are three single peaks between δ 4-4.5 ppm, corresponding to two OMe groups and one NMe group, and two double peaks above δ 7 ppm, reflecting to the aromatic protons (Supplementary data). In the NOESY experiment, one NOE signal was observed between one of Ar-H (peak at 9.38 ppm) and one CH_3 (peak at 4.29 ppm). Another NOE contact was observed between another Ar-H and CH_3 (peaks at 7.90 and 4.16 ppm respectively) (Supplementary data). However, there would have only one NOE signal between Ar-H and CH_3 if the methylation occurs at N2 of the pyridazine. Therefore, it is confirmed to be 3,4-dimethoxy-1-alkylpyridazin-1-ium **16**. From the NOESY experiment, we can also deduce that the chemical shifts at δ 9.38, 7.90, 4.29, 4.16 and 4.07 ppm were assigned respectively to H-6, H-5, NMe, OMe-4 and OMe-3 of compound **16**. Similarly, when compound **14** reacts with ethyl iodide or n-propyl iodide, ethyl and n-propyl groups were found to be attached to the N1 of the pyridazine (see the supplementary data).

Interestingly, the reaction of compounds **14** and **15** with alkyl iodide was strongly influenced by solvent. For example, compound **15** reacts with ethyl iodide in the absence of solvent to form the pyridazinium **17** (Scheme 3). However, when compound **15** was dissolved in acetone before the addition of ethyl iodide, the expected product

Dalton Transactions Accepted Manuscript

pyridazinium **17** was not observed. Instead, a new single spot on TLC occurred between the level of the starting material **15** and the pyridazinium **17**. ^{1}H NMR shows only one methoxy group which is at 3.87 ppm and ESI-MS presents the molecular weight of the new compound at 154 daltons, compared to 169 daltons of the expected product pyridazinium **17**. This new compound was demonstrated to be 1-ethyl-5-methoxypyridazin-4(*1H*)-one **19**. However, when compound **15** was mixed with excess ethyl iodide 5 min before adding acetone, only pyridazinium **17** was obtained. This may be explained by different mechanisms (Scheme 4). In the absence of solvent, the lone pair electrons on the nitrogen of the pyridazine ring can attack the electrophilic alkyl iodide to form pyridazinium. Once the pyridazinium is formed, it is stable and will not undertake further conversions in acetone. In the presence of acetone, however, the breaking of the C-I bond, the formation of a new N-alkyl bond and a new C-I bond occur simultaneously to produce the target pyridazinone (Scheme 4). The produced methyl iodide can be reutilised in the reaction. In reality, we found that when pyridazine **15** reacted with n-propyl iodide in the presence of acetone, a mixture of 1-methyl-5-methoxypyridazin-4(*1H*)-one and 5-methoxy-1-propylpyridazin-4(*1H*)-one (4:1 ratio) was obtained, even with an addition of large excess of n-propyl iodide, reflecting the larger steric hindrance of the propyl group when compared with the methyl group. Similar phenomena were observed for the reaction of compound **14** with alkyl iodides.

Compounds **16** and **17** were de-protected to afford the final metal chelatable bidentate compounds **20** and **21** respectively (Scheme 2). We firstly attempted to use BCl_3 as the de-protecting reagent but incomplete de-protection was observed. We therefore selected stronger de-protecting reagent BBr_3 to carry out this reaction.

Acid dissociation constants and iron(III) affinity constants

The *pKa* values and iron affinity constants for iron(III) of all the pyridazinones are presented in Table 1. The lower pKa_1 value (< 2) is assigned to the protonation of the 4-oxo group and pKa_2 value in the range of 5-7 is assigned to the dissociation of 3- (or 5-) hydroxyl group. Both *pKa* values of the pyridazinones are lower than the corresponding

Dalton Transactions Accepted Manuscript

value for deferiprone. In the group of 3-hydroxypyridazinones **20a-c**, the increase of N-alkyl chain does not dramatically increase the associated *pKa* values. The average pKa_1 and pKa_2 values are at 1.07 and 5.62 respectively. A similar phenomenon was observed for the group of 5-hydroxypyridazinones **21a-c**. However, both the pKa_1 and pKa_2 values of **21a-c** are slightly higher than those of **20a-c**, with average differences at 0.47 and 0.85 respectively. The titration curves for **21a** in the absence and presence of iron is presented in figures 3A and 3B respectively. The corresponding speciation plot indicates that the 3:1 neutral complex dominates over the pH range 6-8 (Fig 4). The lower pKa_2 values of **20a-c** compared with those of **21a-c** indicates the existence of a stronger resonance effect induced by the ortho- nitrogen, which tends to stabilise the 3-oxygen anion.

Due to their higher acid dissociation constants (lower *pKa* values), the iron cumulative stability constants ($\log\beta_3$) and affinity constants (pFe^{3+}) of all the pyridazinones fall correspondingly when compared to the corresponding values for deferiprone (Table 1). In the **20a-c** group, the $\log\beta_3$ value increases with the increase of N-alkyl chain, resulting in an increased pFe^{3+} value. This is in contrast to the **21a-c** group, in which the $\log\beta_3$ and pFe^{3+} values of **21c** are similar to those of **21b**. Significantly both series of compounds were found to possess pFe^{III} values < 20.

Cyclic voltametric analysis and iron(II) affinity constants.

Titration of **20a-c** and **21a-c** in the presence of iron(II) proved to be extremely difficult due to the rapid autoxidation of the iron even when oxygen was exhaustively removed from the system. However reversible redox reactions could be observed by cyclic voltammetry (Fig. 5). The reduction potentials of the various complexes are listed in Table 2. Using these potentials together with the measured $\log\beta_3(Fe^{III})$ values, it was possible to calculate the $\log\beta_3(Fe^{II})$ values (Table 2) and hence the corresponding pFe^{II} values. The K_3 values of this ligands series are relatively low.[13] The pFe^{II} values are all small; a value of 6.0 indicates no binding of iron(II). Clearly **21a** and **21c** bind iron(II) more tightly than **20a-c**, but no pyridazinone was found to bind iron(II) less tightly than deferiprone (**1**).

Dalton Transactions Accepted Manuscript

Conclusions

The aim of this study was to identify a compound with a high selectivity for iron(III) over iron(II), while maintaining a $pFe^{III} \geq 20$. The iron selectivity was compared using $\log\beta_3(Fe^{III})/\log\beta_3(Fe^{II})$. For deferiprone this value is 2.94, with an Fe^{II} $\log\beta_3$ value of 12.4. The affinity for iron(II) is low in both the **20** and **21** series, indeed the extremely low pFe^{II} values for **20** group indicate the these molecules have virtually no binding capacity for iron(II) under physiological conditions (Table 2). However reduction in affinity for iron(II) is reflected in a reduction of affinity for iron(III) and both the **20** and **21** series possess pFe^{III} values < 20. Comparison of $\log\beta_3(Fe^{III})/\log\beta_3(Fe^{II})$ values suggests that the **20** group has marginally higher ratios (mean of **20a**, **20b** and **20c** = 3.00) than that of deferiprone (2.94). Whereas the analogous mean ratio for the **21** group (2.66) was appreciably lower than that of deferiprone. These values compare quite favorably with the corresponding ratios for deferasirox (2.57)[14] and desferatazole (2.26)[15], but confirm the strong position of deferiprone. It appears unlikely that further substitution on the pyridazinone nucleus will facilitate a marked increase of pFe^{III} value to above 20. Deferiprone possesses the optimum differential between the affinities of iron(III) and iron(II), and with a pFe^{II} value of 6.008 does not compete effectively with the iron(II)-glutathione conjugate under likely cytosolic conditions (Fig. 6). Iron(II)-glutathione has been reported to be the major form of labile iron in the cytosol[5, 15]. Thus with typical cytosolic levels of GSH (2 mM) and iron(II) (1 μM), deferiprone (10 μM) does not strongly compete for iron(II) at pH 7.0 (Fig. 6). Even at a deferiprone concentration of 100 μM, competition is relatively weak. Deferiprone chelates approximately 15% of the cytosolic iron, leading to a $([Iron^{II}]\cdot deferiprone)^{+}$ concentration of 1.5×10^{-7}M (Supplementary Data).

Thus deferiprone has close to optimal properties for therapeutic iron chelators and it will be great challenge to further reduce the affinity for iron(II) while maintaining a pFe^{III} value $\geqslant$ 20.

Dalton Transactions Accepted Manuscript

Experimental Section

General Procedures. All chemicals were obtained from Sigma-Aldrich. ^{1}H and ^{13}C-NMR spectra were recorded using a Bruker Avance 400 (400 MHz) NMR spectrometer. Chemical shifts (δ) are reported in ppm downfield from the internal standard tetramethylsilane (TMS). ESI mass spectra were obtained by infusing samples into an LCQ Deca XP ion trap mass instrument. HRMS were monitored on MicroMass Q-TOF instrument. Purity ($\geqslant$95%) was determined via HPLC analysis.

Synthetic procedures

3,4,5-trichloropyridazine (8): A mixture of 4,5-dichloro-3-hydroxypyridazine (16.5 g, 100 mmol) in phosphorus oxychloride (50 ml) was stirred at reflux overnight. $POCl_3$ was removed under reduced pressure and the residue was cooled down by ice bath. Ice water (200 ml) was added into the residue and extracted with dichloromethane (50 ml x 3). The organic layer was washed with brine, dried over Na_2SO_4, evaporated to give the crude product. The crude product was recrystallised with acetone/water to give a white solid Solids were filtered off, washed with water and dried to obtain a white solid (13.8 g, 75%). ^{1}H NMR (400 MHz, $CDCl_3$): δ 9.07 (s, 1H). ESI-MS: m/z=183 $[M+H]^+$.

3,5-dichloro-4-methoxypyridazine (9) and 3,4-dichloro-5-methoxypyridazine (10): Sodium methoxide (25% in MeOH; 10.8 g; 1 equiv.) was added slowly to a solution of 3,4,5-trichloropyridazine (50 mmol) in MeOH (100 ml) at -10°C. The mixture was then stirred at room temperature for 1h. After the solvent was evaporated off under reduced pressure, water (200 ml) was added and extracted three times with dichloromethane (100 ml). The combined organic fractions were dried (Na_2SO_4) and evaporated. The residue was chromatographed (eluent: ethyl acetate:hexane=1:1) to give 3,5-dichloro-4-methoxypyridazine **9** (yield: 32%) from the less polar fraction and 3,4-dichloro-5-methoxypyridazine **10** (yield: 53%) from the polar fraction. ^{1}H NMR ($CDCl_3$) for **9**: δ 9.01 (s, 1H), 4.15 (s, 3H); ^{1}H NMR ($CDCl_3$) for **10**: δ 8.91 (s, 1H), 4.13 (s, 3H).

Dalton Transactions Accepted Manuscript

5-Chloro-3,4-dimethoxypyridazine (11) and 3-chloro-4,5-dimethoxypyridazine (12): monomethoxylated product **9** (3.62 g, 20 mmol) in MeOH (40 ml) was added NaOMe (25% in MeOH, 20 mmol, 1 equiv) and the mixture was refluxed for 1h. After evaporation to remove the solvent, the residue was added water (150 ml) and extracted with dichloromethane (50 ml x 3), dried with Na_2SO_4 and evaporated. The residue was chromatographed on silica gel (eluent: ethyl acetate:hexane=1:1) to give 5-chloro-3,4-dimethoxypyridazine **11** (yield: 40%) from the less polar fraction and 3-chloro-4,5-dimethoxypyridazine **12** (yield: 46%) from the polar fraction. ^{1}H NMR ($CDCl_3$) for **11**: δ 8.71 (s, 1H), 4.19 (s, 3H), 4.11 (s, 3H); ^{1}H NMR ($CDCl_3$) for **12**: δ 8.87 (s, 1H), 4.09 (s, 3H), 4.06 (s, 3H). The compound **12** can also be obtained from monomethoxylation of compound **10** using same procedure as above (yield: 30%).

General procedure for removal of chloride by hydrogeneration: To a solution of 5-chloro-3,4-dimethoxypyridazine or 3-chloro-4,5-dimethoxypyridazine (5 mmol) in ethyl acetate (20 mL), catalytic 20% $Pd(OH)_2/C$ (0.5 g) and triethylamine (10 mmol) were added. The mixture was hydrogenated at room temperature and 3 atms overnight. Then the catalyst was filtered off through celite, and the clear solution, taken to dryness, afforded the title compound. Recrystallisation from a mixture of ethyl acetate and hexane to obtain white crystals.

3,4-Dimethoxypyridazine (14): (yield: 87%). ^{1}H NMR ($CDCl_3$): δ 8.68 (d, J = 5.3 Hz, 1H), 6.75 (d, J = 5.3 Hz, 1H), 4.19 (s, 3H), 3.94 (s, 3H). ESI-MS: m/z=141 $[M+H]^+$.

4,5-Dimethoxypyridazine (15): (yield: 85%). ^{1}H NMR ($CDCl_3$): δ 8.85 (s, 1H), 4.03 (s, 6H). ESI-MS: m/z=141 $[M+H]^+$.

General procedure for preparation of pyridazinium from pyridazine with alkyl iodide: 3,4-Dimethoxy-pyridazine or 4,5-Dimethoxy-pyridazine (10 mmol) in alkyl iodide (10 ml) was stirred at room temperature for 2h. The precipitate was filtrated and washed with acetone to obtain pale yellow crystals.

Dalton Transactions Accepted Manuscript

3,4-Dimethoxy-1-methylpyridazinium iodide (16a): (yield: 84%). ^{1}H NMR (d_6-DMSO): δ 9.15 (d, J = 6.6 Hz, 1H), 7.67 (d, J = 6.6 Hz, 1H), 4.06 (s, 3H), 3.93 (s, 3H), 3.85 (s, 3H). ESI-MS: m/z=155 $[M+H]^+$.

4,5-Dimethoxy-1-methylpyridazinium iodide (17a): (yield: 80%). ^{1}H NMR (d_6-DMSO): δ 9.57 (s, 1H), 9.18 (s, 1H), 4.35 (s, 3H), 4.14 (s, 3H), 3.99 (s, 3H). ESI-MS: m/z=155 $[M+H]^+$.

General procedure for preparation of pyridazin-4-ones: 3,4-Dimethoxy-pyridazine or 4,5-Dimethoxy-pyridazine (10 mmol) was dissolved in acetone (20 ml). Alkyl iodide (15 mmol) was added to the solution and the mixture was stirred at 50°C for 20h. After removal of the solvent under reduced pressure, the residue was purified by column chromatography (eluent: EtOAc:MeOH=9:1) to obtain target compounds.

3-Methoxy-1-methylpyridazin-4(1*H*)-one (18a): (yield: 92%). ^{1}H NMR ($CDCl_3$): δ 7.68 (d, J = 7.2 Hz, 1H), 6.32 (d, J = 7.2 Hz, 1H), 3.91 (s, 3H), 3.83 (s, 3H). ESI-MS: m/z=141 $(M+1)^+$.

1-Ethyl-3-methoxypyridazin-4(1*H*)-one (18b): (yield: 63%). ^{1}H NMR ($CDCl_3$): δ 7.75 (d, J = 7.1 Hz, 1H), 6.38 (d, J = 7.1 Hz, 1H), 4.03 (q, J = 7.3 Hz, 2H), 3.94 (s, 3H), 1.49 (t, J = 7.3 Hz, 3H). ESI-MS: m/z=155 $(M+1)^+$.

3-Methoxy-1-propylpyridazin-4(1*H*)-one (18c): (yield: 18%). ^{1}H NMR ($CDCl_3$): δ 7.72 (d, J = 7.1 Hz, 1H), 6.40 (d, J = 7.1 Hz, 1H), 3.94 (s, 3H), 3.92 (t, J = 7.0 Hz, 2H), 1.94-1.86 (m, 2H), 0.95 (t, J = 7.4 Hz, 3H). ESI-MS: m/z=169 $(M+1)^+$.

1-Ethyl-5-methoxypyridazin-4(1*H*)-one (19b): (yield: 65%). ^{1}H NMR ($CDCl_3$): δ 7.92 (s, 1H), 7.63 (s, 1H), 4.16 (q, J = 7.3 Hz, 2H), 3.87 (s, 3H), 1.51 (t, J = 7.3 Hz, 3H). ESI-MS: m/z=155 $(M+1)^+$.

5-Methoxy-1-propylpyridazin-4(1*H*)-one (19c): (yield: 15%). ^{1}H NMR ($CDCl_3$): δ 7.93 (s, 1H), 7.49 (s, 1H), 4.06 (t, J = 7.2 Hz, 2H), 3.87 (s, 3H), 1.95-1.89 (m, 2H), 0.97 (t, J = 7.4 Hz, 3H). ESI-MS: m/z=169 $(M+1)^+$.

Dalton Transactions Accepted Manuscript

General procedure for deprotection of hydroxyl group on pyridaziniums or pyridazin-4-ones: Dichloromethane (anhydrous, 20 ml) was added to the methoxy substituted pyridaziniums or pyridazin-4-ones (2 mmol) and flushed with nitrogen. Boron tribromide (1 M in dichloromethane, 8 mL) was slowly added and the reaction mixture was stirred at room temperature for one day. The excess BBr_3 was eliminated at the end of the reaction by the addition of methanol (10 mL) and left to stir for another half an hour. After removal of the solvents under reduced pressure, the residues were purified by recrystallization to afford a white solid

3-Hydroxyl-1-methylpyridazin-4(1*H*)-one (20a): (yield: 62%). ^{1}H NMR (d_6-DMSO): δ 9.32 (d, J = 6.4 Hz, 1H), 7.70 (d, J = 6.4 Hz, 1H), 5.02 (brs, OH), 4.26 (s, 3H). ^{13}C NMR (d_6-DMSO): δ 49.81, 108.61, 147.77, 154.40, 159.75. HRMS: Calcd for $C_5H_7N_2O_2$ $(M+1)^+$, 127.0508; Found, 127.0514.

1-Ethyl-3-hydroxypyridazin-4(1*H*)-one (20b): (yield: 68%). ^{1}H NMR (d_6-DMSO): δ 8.78 (d, J = 6.6 Hz, 1H), 8.46 (brs, OH), 6.98 (d, J = 6.6 Hz, 1H), 4.27 (q, J = 7.2 Hz, 2H), 1.41 (t, J = 7.2 Hz, 3H). ^{13}C NMR (d_6-DMSO): δ 14.64, 55.81, 112.66, 143.11, 157.52, 159.65. HRMS: Calcd for $C_6H_9N_2O_2$ $(M+1)^+$, 141.0664; Found, 141.0653.

3-Hydroxyl-1-propylpyridazin-4(1*H*)-one (20c): (yield: 66%). ^{1}H NMR (d_6-DMSO): δ 8.79 (d, J = 6.6 Hz, 1H), 8.15 (brs, OH), 6.99 (d, J = 6.6 Hz, 1H), 4.20 (t, J = 6.9 Hz, 2H), 1.89-1.74 (m, 2H), 0.86 (t, J = 7.4 Hz, 3H). ^{13}C NMR (d_6-DMSO): δ 10.26, 22.26, 61.79, 112.50, 143.59, 157.57, 159.67. HRMS: Calcd for $C_7H_{11}N_2O_2$ $(M+1)^+$, 155.0820; Found, 155.0843

5-Hydroxyl-1-methylpyridazin-4(1*H*)-one (21a): (yield: 70%). ^{1}H NMR (d_6-DMSO): δ 10.22 (brs, OH), 8.93 (s, 1H), 8.56 (s, 1H), 4.23 (s, 3H). ^{13}C NMR (d_6-DMSO): δ 49.45, 136.37, 142.04, 148.77, 153.52. HRMS: Calcd for $C_5H_7N_2O_2$ $(M+1)^+$, 127.0508; Found, 127.0504.

1-Ethyl-5-hydroxylpyridazin-4(1*H*)-one (21b): (yield: 66%). ^{1}H NMR (d_6-DMSO): δ 8.93 (s, 1H), 8.54 (s, 1H), 4.46 (t, J = 7.3 Hz, 2H), 4.31 (brs, OH), 1.45 (t, J = 7.3 Hz,

Dalton Transactions Accepted Manuscript

3H). ^{13}C NMR (d_6-DMSO): δ 14.80, 57.36, 135.57, 142.26, 148.92, 153.62. HRMS: Calcd for $C_6H_9N_2O_2$ $(M+1)^+$, 141.0664; Found, 141.0655.

5-Hydroxyl-1-propylpyridazin-4(1*H*)-one (21c): (yield: 69%). ^{1}H NMR (d_6-DMSO): δ 9.89 (brs, OH), 8.99 (s, 1H), 8.58 (s, 1H), 4.42 (t, J = 7.1 Hz, 2H2), 1.93-1.83 (m, 2H), 0.87 (t, J = 7.4 Hz, 3H). ^{13}C NMR (d_6-DMSO): δ 10.29, 22.75, 63.16, 135.59, 142.27, 148.89, 153.96. HRMS: Calcd for $C_7H_{11}N_2O_2$ $(M+1)^+$, 155.0820; Found, 155.0816.

Spectrophotometric method for pKa and iron stability constant determinations:

The automatic titration system used in this study comprised an autoburette (Metrohm Dosimat 765 liter ml syringe) and Mettler Toledo MP230 pH meter with Metrohm pH electrode (6.0133.100) and a reference electrode (6.0733.100). 0.1 M KCl electrolyte solution was used to maintain the ionic strength. The temperature of the test solutions was maintained in a thermostatic jacketed titration vessel at 25°C ± 0.1°C by using a Techne TE-8J temperature controller. The pH meter was calibrated through titrating a volumetric standard, strong acid HCl (0.160 mL, 0.2 M) in KCl (20mL 0.1M) with KOH (0.1 M) under an argon gas atmosphere at 25°C. The volume of base added and the electrode potential were recorded at each point. A Gran plot was generated using GLEE[17] (Glass Electrode Evaluation) and the obtained numbers (E_0, Slope of electrode, and CO_2 concentration) were used for corrections. The solution under investigation was stirred vigorously during the experiment. A Gilson Mini-plus#3 pump with speed capability (20 ml/min) was used to circulate the test solution through a Hellem quartz flow cuvette. For the stability constant determinations, a 50 mm path length cuvette was used, and for *pKa* determinations, a cuvette path length of 10 mm was used. The flow cuvette was mounted on an HP 8453 UV-visible spectrophotometer. All instruments were interfaced to a computer and controlled by a Visual Basic program. Automatic titration and spectral scans adopted the following strategy: the pH of a solution was increased by 0.1 pH unit by the addition of KOH from the autoburette; when pH readings varied by <0.001 pH unit over a 3 s period, an incubation period was activated. For *pKa* determinations, a period of 0.1 min was adopted; for stability constant determinations, a period of 10-30 min was adopted. At the end of the equilibrium period, the spectrum of the solution was

Dalton Transactions Accepted Manuscript

then recorded. The cycle was repeated automatically until the defined end point pH value was achieved. All the titration data were analyzed with the pHab program.[18] The species plot was calculated with the HYSS program.[19] Analytical grade reagent materials were used in the preparation of all solutions.

Electrochemical Measurements:

Cyclic voltammetry (CV) measurements were performed with a CS-120 device (Corrtest). All complexes (iron(III), 1mM; ligand, 5mM) at pH 7.42 (0.2M MOPS) were prepared. All measurements were conducted under N_2 in a jacketed, one-compartment cell with a Hg working electrode (Corrtest), a platinum wire counter electrode (Corrtest) and a Ag/AgCl reference electrode. The sweep rate was 100 mV/s.

O_2 was removed from the electrolyte solution by bubbling N_2 through the solvent for several minutes prior to making the measurement. A N_2 atmosphere was continuously maintained above the solution while the experiments were in progress. The temperature was controlled by using a double-jacketed cell and a thermostat with water bath at 25 ^{o}C.

Acknowledgements

The authors would like to thank Apotex Research Inc Canada for supporting this research project.

References:

1. Y. Ma, T. Zhou, X. Kong and R. C. Hider, *Curr. Med. Chem.*, 2012, 19, 2816-2827.
2. T. F. Tam, R. Leung-Toung, W. Li, Y. Wang, K. Karimian and M. Spino, *Curr. Med. Chem.*, 2003, 10, 983-995.
3. E. G. Kovaleva and J. D. Lipscomb, *Nat. Chem. Biol.*, 2008, 4, 186-193.
4. C. Loenarz and C. J. Schofield, *Nat. Chem. Biol.*, 2008, 4, 152-156.
5. R. C. Hider and X. Kong, *Dalton Trans*, 2013, 42, 3220-3229.
6. A. Ozer and R. K. Bruick, *Nat. Chem. Biol.*, 2007, 3, 144-153.
7. W. Breuer, S. Epsztejn and Z. I. Cabantchik, *J. Biol. Chem.*, 1995, 270, 24209-24215.
8. Y. Ma, H. de Groot, Z. Liu, R. C. Hider and F. Petrat, *Biochem J*, 2006, 395, 49-55.
9. G. Zanninelli, O. Loreal, P. Brissot, A. M. Konijn, I. N. Slotki, R. C. Hider and Z. Ioav Cabantchik, *J Hepatol*, 2002, 36, 39-46.
10. C. Hershko, A. M. Konijn and G. Link, *Br J Haematol*, 1998, 101, 399-406.
11. Z. D. Liu and R. C. Hider, *Med. Res. Rev.*, 2002, 22, 26-64.
12. H. Nagashima, H. Oda, J. Hida and K. Kaji, *Chem. Pharm. Bull.*, 1987, 35, 421-424.

Dalton Transactions Accepted Manuscript

13. M. Merkofer, A. Domazou, T. Nauser and W. H. Koppend, *Eur. J. Inorg. Chem.*, 2006, 671-675.
14. S. Steinhauser, U. Heinz, M. Bartholoma, T. Weyhermuller, H. Nick and K. Hegetschweiler, *Eur. J. Inorg. Chem.*, 2004, DOI: 10.1002/ejic.200400363, 4177-4192.
15. X. Kong. R. Hider, T. Luker, K. Conlon and R. Harland, presented in part at the 55th ASH Annual Meeting and Exposition, New Orleans, LA, 2013.
16. R. C. Hider and X. L. Kong, *Biometals*, 2011, 24, 1179-1187.
17. P. Gans and B. O'Sullivan, *Talanta*, 2000, 51, 33-37.
18. P. Gans, A. Sabatini and A. Vacca, *Annali Di Chimica*, 1999, 89, 45-49.
19. L. Alderighi, P. Gans, A. Ienco, D. Peters, A. Sabatini and A. Vacca, *Coord. Chem. Rev*, 1999, 184, 311-318.
20. G. Xiao, D. van der Helm, R. C. Hider and P. S. Dobbin, *J. Chem. Soc., Dalton Trans.*, 1992, 3265-3271.
21. C. F. Baes and R. E. Mesmer, *The hydrolysis of cations*, John Wiley & Sons, New York., 1976.

Dalton Transactions Accepted Manuscript

Table 1 *pKa* values and iron(III) affinity constants of pyridazinones.

ID	structure	pKa_1	pKa_2	$LogK_1$	$Log\beta_2$	$Log\beta_3$	pFe^{3+}
deferiprone	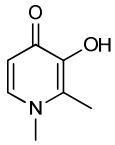	3.68	9.77	14.6	26.8	36.4	20.6
20a	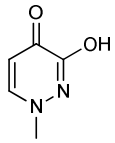	1.1	5.56	9.6	17.2	23.2	14.8
20b	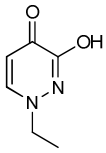	1.1	5.63	8.3	16.9	23.8	14.9
20c	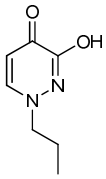	1.0	5.66	8.5	17.5	24.8	15.5
21a	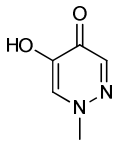	1.5	6.44	10.2	19.3	26.8	17.2
21b	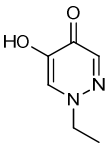	1.5	6.47	10.3	19.4	27.1	17.5
21c	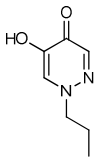	1.5	6.54	10.4	19.5	27.1	17.5

Dalton Transactions Accepted Manuscript

Table 2 Reduction potentials and iron(II) affinity constants

ID	$\log\beta_3(Fe^{II})$	$\log\beta_3(Fe^{III})$	E_0	pFe^{III}	pFe^{II}	$\log\beta_3(Fe^{III})/\log\beta_2(Fe^{II})$
deferiprone	12.4	36.4	-620	20.6	6.008	2.94
20a	7.4	23.2	-165	14.8	6.011	3.14
20b	7.93	23.8	-169	14.9	6.014	3.00
20c	8.7	24.8	-182	15.5	6.024	2.85
21a	10.05	26.8	-221	14.7	6.065	2.67
21b	N.D.	27.1	N.D.	16.3	N.D.	N.D.
21c	10.33	27.1	-222	16.1	6.081	2.62

Note: pFe^{III} values are for pH 7.4, $[Fe]_{total}$ = 1 μM and $[ligand]_{total}$ = 10 μM; and pFe^{II} values are for pH 7.4, $[Fe]_{total}$ = 1 μM and $[ligand]_{total}$ = 100 μM.

E_0—reduction potential (vs NHE) for Fe^{III}/Fe^{II} in presence of five-fold molar excess of ligand.

N.D. Not Determined.

Using the E_0 value and the $\log\beta_3$ value for iron(III), the $\log\beta_3$ value for iron(II) was calculated from the following equation:
$(\log\beta_3 Fe^{3+} - \log\beta_3 Fe^{2+}) = E_0(Fe^{3+}/Fe^{2+}) - E_{complex}(Fe^{3+}/Fe^{2+})$, where $E_0(Fe^{3+}/Fe^{2+})$ is the redox potential of the iron pair in the absence of the ligand (+770mV) and $E_{complex}$-(Fe^{3+}/Fe^{2+}) is the redox potential in the presence of the ligand.

Dalton Transactions Accepted Manuscript

Legends of Figures

Figure 1: Calculated 3D pFe^{2+} surface with varying *pKa* (5 – 10) and logβ_3 values (6 – 14) at pH 7.4 of a hypothetical ligand when $[Fe^{2+}]_{total}$ =1 μM, $[L]_{total}$ =100 μM. Ideally we wish to identify a ligand with properties that fall in the lower right hand region of the plot. The data was generated by HYSS.[19]

Figure 2: Molecular structure of 3:1 $(DFP)_3$:Fe complex (**4**). Space filled structure based on x-ray diffraction[20].

Figure 3: pH-dependent UV/Vis spectra of **21a** over the range of pH 2.1-12.1. A) Experiment with [**21a**]= 110.3 μM in 12.033 ml 0.1 M KCl at 25 ^{o}C, pH from 2.1 to pH 12.1; B) Experiment with [**21a**]= 147.2 μM, $[Fe^{III}]$= 33.6 μM (ratio of L:M= 4.4) in 15.033 ml 0.1M KCl at 25 ^{o}C, pH from 1.965 to pH 8.082.

Figure 4: Speciation plot of iron(III) in the presence of **21a**: $[Fe]_{total}$ = 1 μM, $[\mathbf{21a}]_{total}$ = 10 μM using the iron hydroxide constant at FeOH (-2.563), $Fe(OH)_2$ (-6.205), $Fe(OH)_3$ (-15.1), $Fe(OH)_4$ (-21.883) and $Fe_2(OH)_2$(-2.843)[21].

Figure 5: Cyclic voltammetry of the iron complexes of deferiprone (**1**) and **21a** at pH 7.4. [Fe] = 1mM; [ligand] = 5 mM.

Figure 6: Speciation plot of iron(II) in the presence of deferiprone and glutathione. $[Fe]_{total}$ = 1 μM, $[Deferiprone]_{total}$ = 10 μM, $[GSH]_{total}$ = 2 mM; $logK_1$ for iron(II)GS = 5.1.[16]

Dalton Transactions Accepted Manuscript

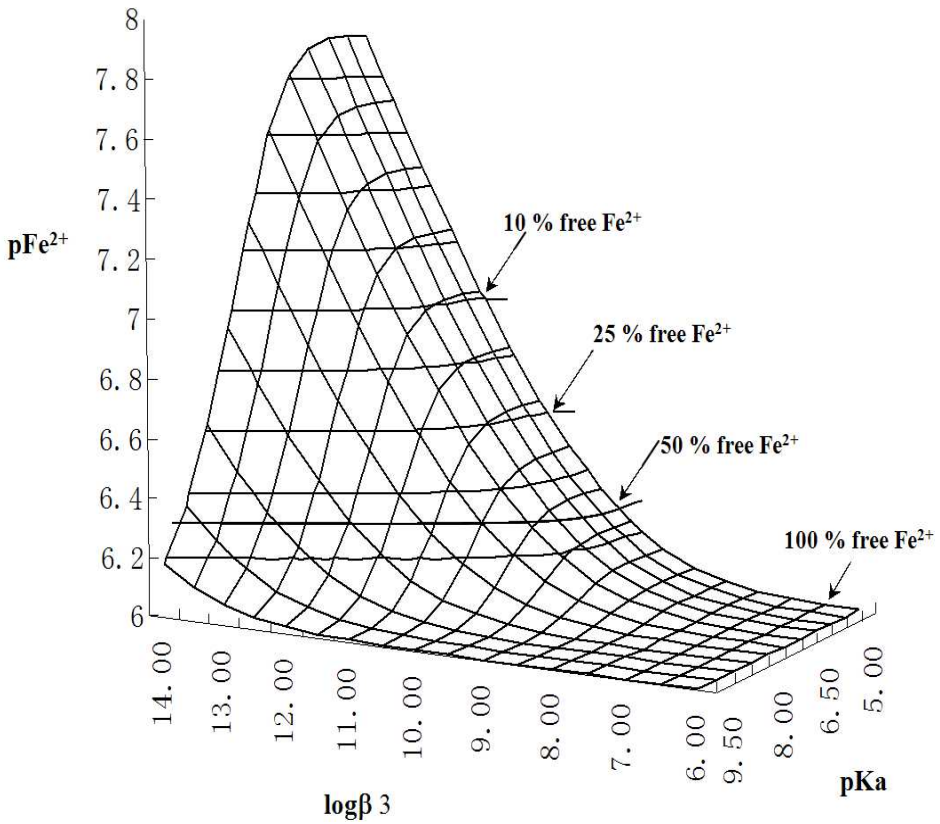

Figure 1

Dalton Transactions Accepted Manuscript

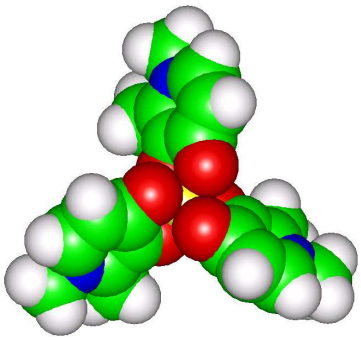

Figure 2

Dalton Transactions Accepted Manuscript

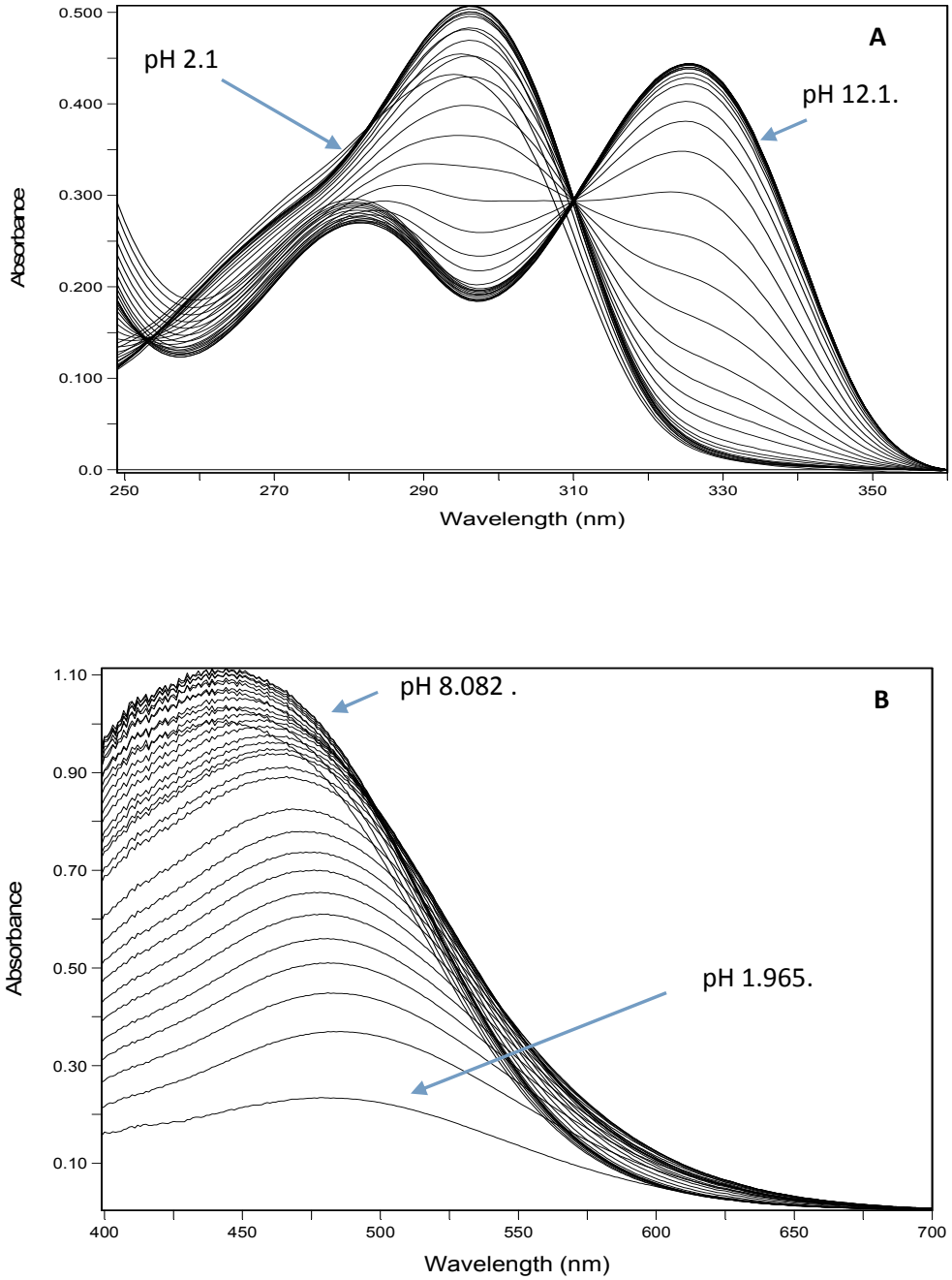

Figure 3

Dalton Transactions Accepted Manuscript

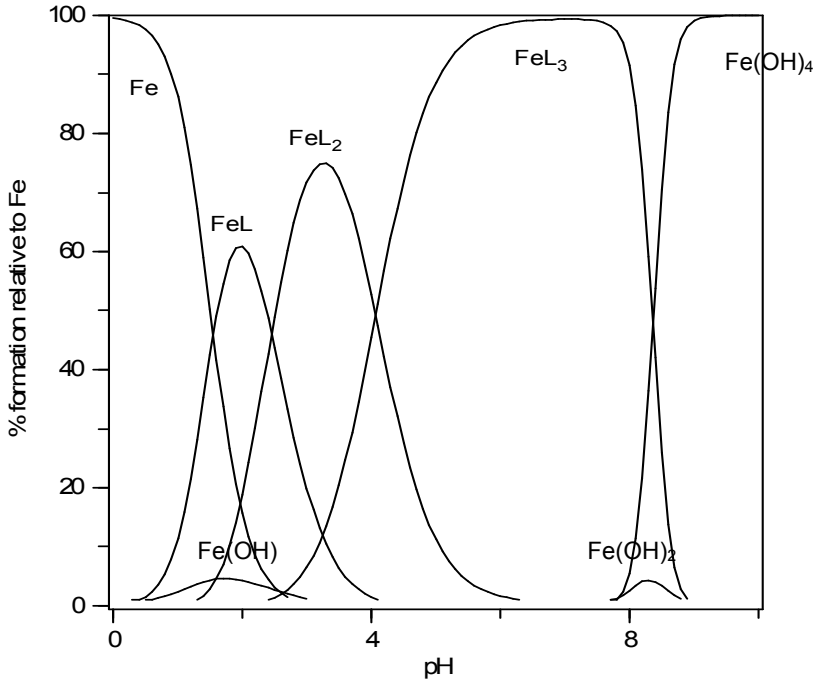

Figure 4

Dalton Transactions Accepted Manuscript

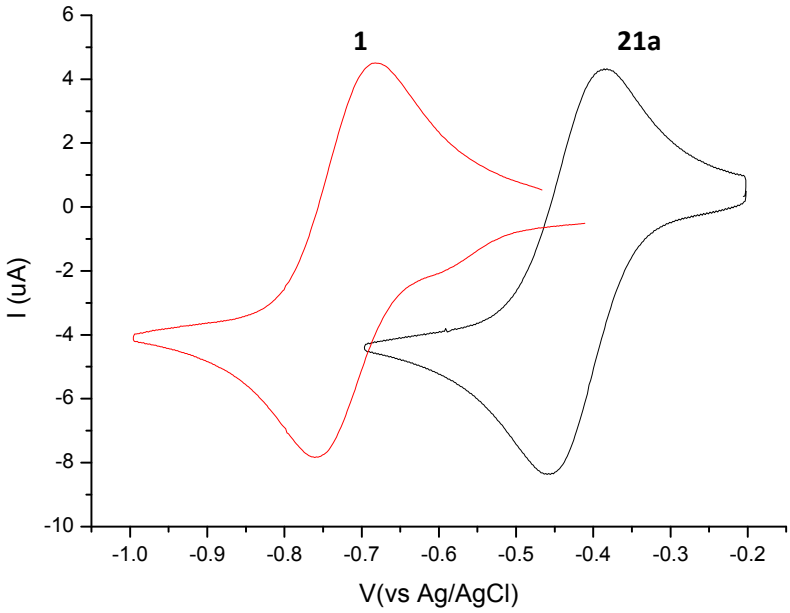

Figure 5

Dalton Transactions Accepted Manuscript

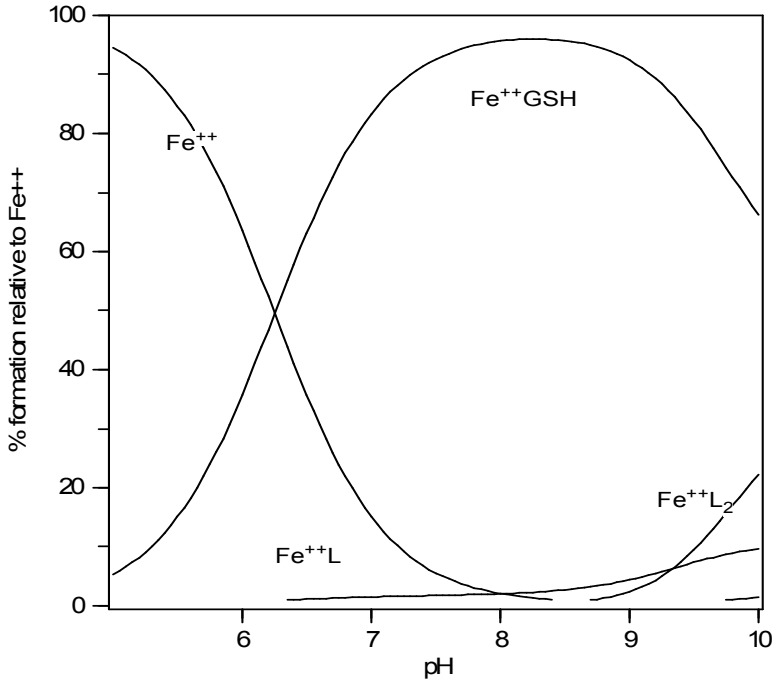

Figure 6

Dalton Transactions Accepted Manuscript

Scheme 1: Two resonance forms of deferiprone (**1**) and pyridazinone (**2** and **3**).

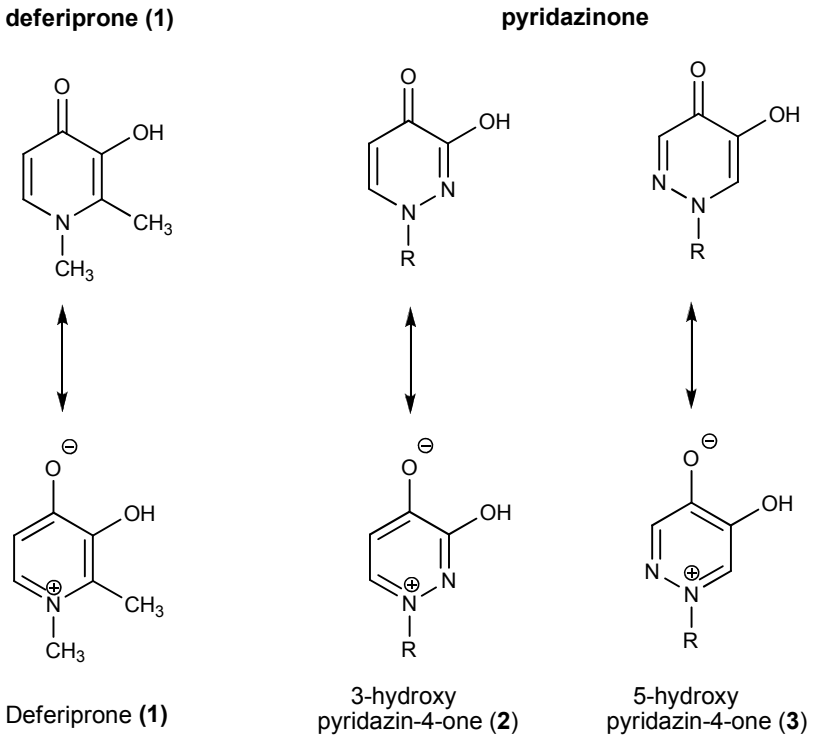

Dalton Transactions Accepted Manuscript

Scheme 2: Synthesis of 3(5)-hydroxyl-1-alkylpyridazin-4(*1H*)-one. a) NaOMe, reflux; b) K_2CO_3/MeI, reflux; c) $POCl_3$, reflux overnight; d) NaOMe/-10 ^oC, 1 h; e) NaOMe, reflux in MeOH, 1 h; f) $Pd(OH)_2/H_2$, 30 psi, overnight; g) alkyl iodide in the presence or absence of acetone; h) BBr_3/CH_2Cl_2, overnight.

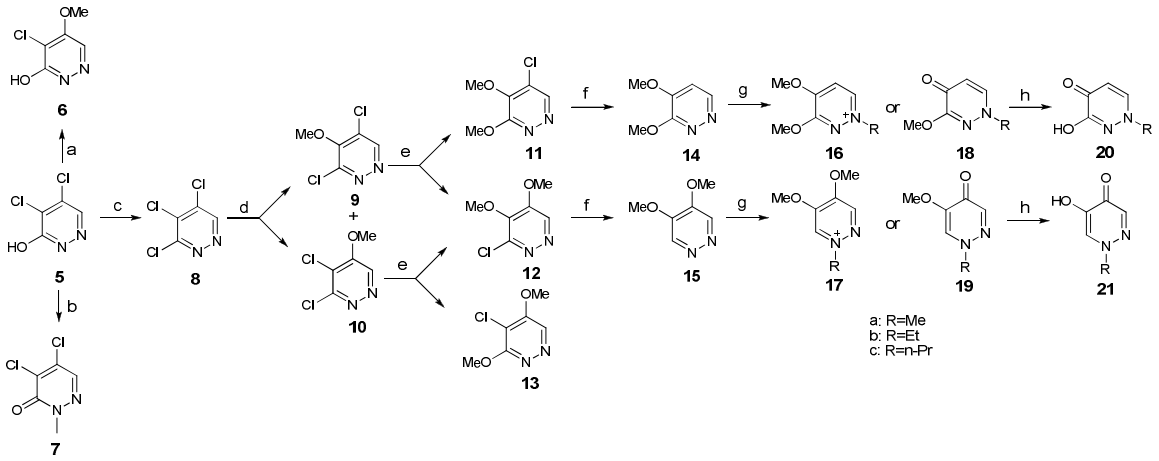

Dalton Transactions Accepted Manuscript

Scheme 3: Synthesis of pyridazinone and pyridazinium. a) RI, overnight; b) in acetone added RI, overnight.

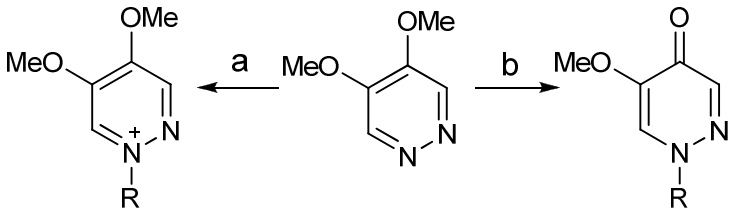

17 **15** **19**

Dalton Transactions Accepted Manuscript

Scheme 4: Possible mechanism for conversion of pyridazine to pyridazinium and pyridazinone.

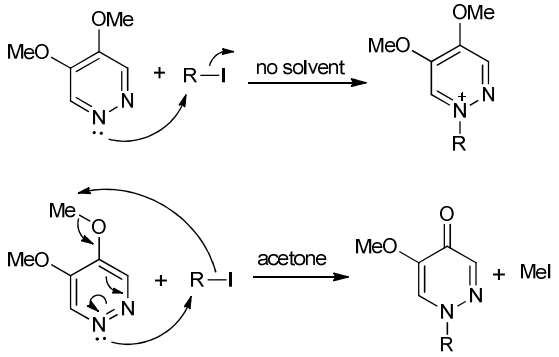

Dalton Transactions Accepted Manuscript